

## Angular Velocity Sensor Using Winking Phenomenon in Solid-State Ring Resonator

Taichi Hashimoto<sup>1,2,\*</sup>, Kenichi Makimura<sup>1</sup>, Kensuke Kanda<sup>1,2</sup>,  
Takayuki Fujita<sup>1,2</sup> and Kazusuke Maenaka<sup>1,2</sup>

<sup>1</sup>Graduate School of Engineering, University of Hyogo, 2167 Shosha, Himeji 671-2280, Japan

<sup>2</sup>Maenaka Human-Sensing Fusion Project, Japan Science and Technology Agency,  
2167 Shosha, Himeji 671-2280, Japan

(Received April 25, 2011; accepted June 23, 2011)

**Key words:** winking phenomenon, ring laser gyroscope, semiconductor optical amplifier

In this paper, we describe a novel type of ring laser gyroscope (RLG) using the winking phenomenon. Conventional sensing methods of gyroscopes are categorized into vibrating-type gyroscopes using the Coriolis force and optical-type gyroscopes using the Sagnac effect. The novel type of gyroscope presented here utilizes the winking phenomenon. The winking phenomenon is intensity changes of circulatory counter propagating lasers with an applied angular velocity. The advantage is that the intensity change caused by the winking phenomenon is more than 100 times larger than the capacitance change of conventional gyroscopes in micro-electromechanical systems (MEMS) technology. The detecting circuits for the winking phenomenon become simple compared with the vibrating MEMS gyroscope, because the circuits of the MEMS gyroscopes should detect a capacitance change of  $1.5 \times 10^{-4} \%$ /deg/s, which corresponds to 0.7 aF/deg/s. The novel RLG using the winking phenomenon does not have a dead-band because the intensity changes are linearly observed at a small to middle angular velocity. Thus, a mechanical dither is not required like in a conventional RLG using a He-Ne laser. In the experiments, an RLG including a semiconductor optical amplifier (SOA), mirrors, and beam splitters is assembled to observe the winking phenomenon. The basic characteristics of laser intensity vs. injection current and wavelength spectra were confirmed and the winking phenomenon was observed when an angular velocity was applied to the RLG. We observed that the change in laser intensity is  $1.9 \times 10^{-2} \%$ /deg/s.

---

\*Corresponding author: e-mail: eu09r001@steng.u-hyogo.ac.jp

## 1. Introduction

In recent years, gyroscopes, which detect an angular velocity, have been miniaturized using micro-electromechanical systems (MEMS) technology.<sup>(1)</sup> The advantages of the MEMS gyroscopes are their small size, low cost, and medium resolution of 0.01–0.1 deg/s Hz<sup>-1/2</sup>.<sup>(2)</sup> The MEMS gyroscopes are widely used for vibration reduction systems of digital cameras, game controllers, and navigation systems of automobiles. Commonly, the MEMS gyroscopes are vibration type, in which they have vibrating masses and capacitance sensing electrodes. When an angular velocity is applied, the masses move to the electrodes by the Coriolis force and then the electrostatic capacitance change at the electrodes becomes the output of the device. However, the capacitance change of the conventional MEMS gyroscopes is extremely low (femto- or atto-farad order).<sup>(3–6)</sup> For example, an initial capacitance and capacitance change by the applied angular velocity in ADXRS300 (Analog Devices Inc.) are 460 fF and 0.7 aF/deg/s, respectively. The detecting circuit should detect a capacitance change of  $1.5 \times 10^{-4} \%$ /deg/s. So, the detecting circuits (capacitance/voltage (C/V) converters, amplifiers, etc.) should be designed with the greatest caution to measure such a small change, and also the assembly technology for the sensor structure and the circuitry should be limited — long or mechanically weak wiring between the sensor structure and the circuit is not allowed. Resulting from these critical issues, the absolute characteristics, especially the bias stability, are limited for current MEMS gyroscopes.

Although almost all MEMS gyroscopes use the Coriolis force, conventional optical-type gyroscopes such as fiber optic gyroscopes (FOGs) and ring laser gyroscopes (RLGs) are based on the Sagnac effect.<sup>(7)</sup> Optical gyroscopes require counter propagating lasers in a closed optical loop, which is provided by a coiled long optical fiber or an area enclosed by mirrors. The Sagnac effect in the conventional optical gyroscopes generates the changes in the wavelength or phase of counter propagating lasers when an angular velocity is applied. The RLGs are used in inertial navigation systems of planes and ships, etc., because of their high bias stability (about 0.04 deg/h).<sup>(8)</sup> However, the RLGs are large and heavy, have a high power consumption, and are expensive because He-Ne gas is used as the gain medium and special glasses and mirrors are used for optical components.

Lock-in and winking phenomena are unique features of the RLGs.<sup>(9,10)</sup> The wavelengths of the RLGs are ideally changed by the applied angular velocity according to the Sagnac effect. However, when the applied angular velocity is small, the wavelengths of propagating lasers are not changed. This phenomenon is known as the lock-in.<sup>(7)</sup> When the RLG is in lock-in state, the intensities of counter propagating lasers are differentially changed depending on the applied angular velocity.<sup>(9)</sup> This intensity change is known as the winking phenomenon. There is a possibility that the winking phenomenon may be used as a sensing mechanism of the angular velocity because the intensity change caused by the winking phenomenon is much larger than the capacitance change caused by the mass movement of the MEMS vibrating gyroscopes.

In this paper, we propose a novel type of RLG, which senses angular velocity by using the winking phenomenon. It has the following advantages: (1) the sensitivity

of the applied angular velocity is much larger than that of the MEMS gyroscopes, (2) complex circuits, such as a C/V converter that senses the small capacitance change, are not needed, (3) high-performance mirrors and accurate machining are not needed compared with conventional RLGs because some backscattering in the mirrors is allowed, as described later, and (4) mechanical dither is not required because the winking phenomenon can be observed from a static state to a medium applied angular velocity. To investigate the feasibility of the gyroscope exploiting the winking phenomenon, a commercial semiconductor optical amplifier (SOA) and mirrors forming a ring resonator were combined and the winking phenomenon was observed. In this paper, we report the basic characteristics of laser oscillation with the SOA as the gain medium, observation of winking phenomenon, and the stability of the RLG.

## 2. Principle and Winking Phenomenon

### 2.1 Conventional ring laser gyroscope

Figure 1 shows a schematic of a conventional RLG.<sup>(6)</sup> He-Ne gas is encapsulated in the narrow cavity made of a nonthermal expansion glass. The He-Ne gas is excited and discharged between the anodes and cathodes. Since the lights are reflected by mirrors, the lights are optically amplified by the gain medium of the excited He-Ne gas in the cavity. Then, oppositely propagating clockwise (CW) and counter-clockwise (CCW)

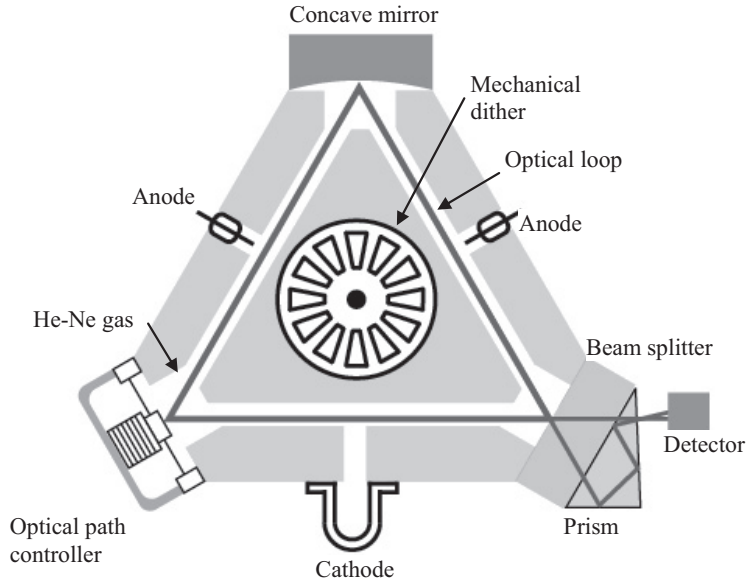


Fig. 1. Schematic of typical structure of a conventional RLG.

laser beams are simultaneously generated. The laser beams are fed through the beam splitter and mixed at the detector, and a fringe pattern is generated. When an angular velocity  $\Omega$  is applied, the fringe pattern moves at beat frequency  $f$ .  $f$  is given by

$$f = \frac{4S}{L\lambda} \Omega, \quad (1)$$

where  $S$  is the area surrounded by the optical loop shown in Fig. 1,  $L$  is the optical path length, and  $\lambda$  is the oscillating wavelength.

## 2.2 Lock-in

The beat frequency caused by the Sagnac effect is ideally proportional to the applied angular velocity, as shown by the dashed line in Fig. 2. However, when the applied angular velocity is small, the frequency is fixed to zero. The beat frequency can be observed when the angular velocity becomes large. This phenomenon is known as the lock-in, and the angular velocity threshold is known as the lock-in threshold.<sup>(7)</sup> In the RLG, two opposite propagating laser beams travel in the optical loop. A small part of the laser beams is scattered by the mirrors because the mirrors have imperfections even if they are high reflection mirrors of 99.99% or more. The scattered laser beams propagate to the opposite direction. The counter propagating laser and the scattered laser beams are intermixed. Therefore, wavelengths are pulled-in and lock-in occurs. Usually, the lock-in is an inevitable characteristic. To overcome this problem, mechanical dither, which applies an alternative angular velocity (larger than the lock-in threshold), is used to sense a small angular velocity within the lock-in threshold.

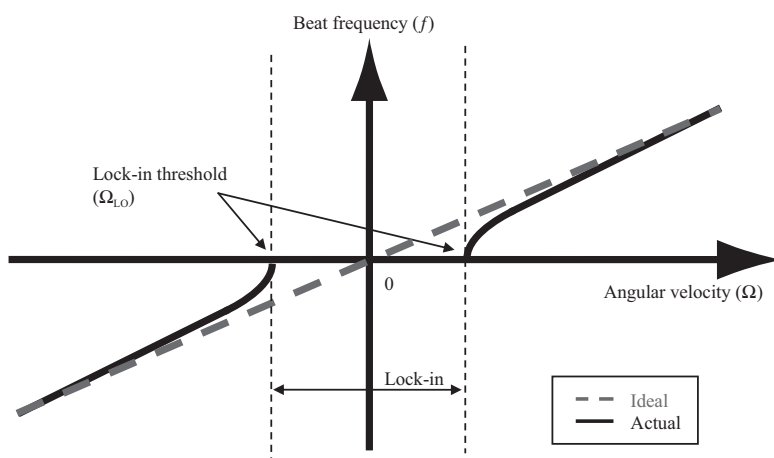


Fig. 2. Sagnac beat output signal.

### 2.3 Winking phenomenon

The winking phenomenon was reported by Aronowitz and Collins in 1970<sup>(9)</sup> and Kataoka and Kawahara in 1986.<sup>(10)</sup> The winking phenomenon is the intensity change of laser beams in the lock-in state depending on the applied angular velocity, and it originates from the Sagnac effect. The typical features are as follows: (1) the intensity changes are differential between the CW and CCW lasers. (2) If the applied angular velocity is in the CW direction, the intensity of the CW laser beam decreases. (3) The changes are almost linear until the lock-in threshold. When the angular velocity becomes larger than the lock-in threshold, the intensities become zero rate intensities asymptotically. The origin of the winking phenomenon is the backscattering, the same as for the lock-in. The typical intensity changes caused by winking phenomenon are shown schematically in Fig. 3.

The intensity change caused by the winking phenomenon is given by<sup>(9)</sup>

$$I'_1 = (c/L)I_1[\alpha_1 - \beta_1 I_1 - \theta_{12} I_2 + 2r_2(I_2/I_1)\cos(\varphi + \varepsilon)], \quad (2)$$

$$I'_2 = (c/L)I_2[\alpha_2 - \beta_2 I_2 - \theta_{21} I_1 + 2r_1(I_1/I_2)\cos(\varphi - \varepsilon)], \quad (3)$$

$$\varphi = \sin^{-1}(\Omega/\Omega_{LO}), \quad (4)$$

$$\Omega_{LO} = 2(r_1 r_2)^{1/2} \cos \varepsilon, \quad (5)$$

where  $I_1, I_2$  are the laser intensities at zero rate,  $I'_1, I'_2$  are the laser intensities at the applied angular velocity,  $c$  is the velocity of light,  $L$  is the optical path length,  $\alpha_1, \alpha_2$  are the gain minus losses,  $\beta_1, \beta_2$  are the saturation effects based on a spontaneous emission,

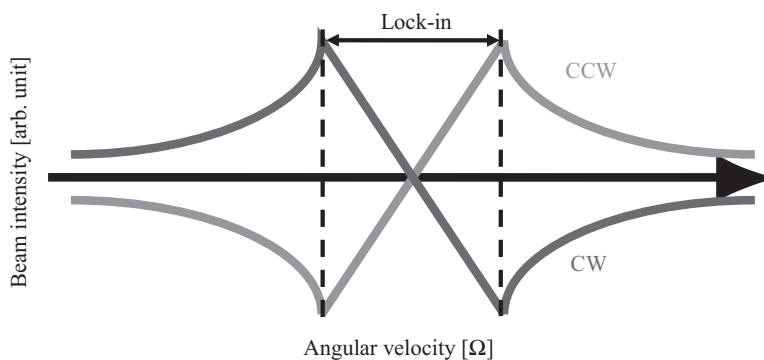


Fig. 3. Typical winking patterns.

$\theta_1$ ,  $\theta_2$  are the mutual saturation effects when one laser intensity decreases and the gain of the other laser increases,  $r_1$ ,  $r_2$  are the backscattering coefficients of mirrors,  $\varepsilon$  is the summation of phases when lasers are backscattered by the mirrors,  $\Omega$  is the applied angular velocity, and  $\Omega_{LO}$  is the angular velocity of the lock-in threshold. The suffixes 1 and 2 correspond to the beams in the CW and CCW directions. If the  $I$ ,  $c$ ,  $L$ ,  $\alpha$ ,  $\beta$ ,  $\theta$ ,  $r$ , and  $\varepsilon$  are assumed to be constant values,  $I$  depends on  $\Omega$ . To reduce the lock-in threshold,  $r_1$  and  $r_2$  should be extremely reduced, and severe control of  $\varepsilon$  is required.

Generally, miniaturizing the total size of gyroscopes, the sensitivity decreases because miniaturization of their size decreases the mass movement caused by the Coriolis force. In the RLG sensing with the winking phenomenon, there is a possibility that the intensity changes of laser beams may increase by the miniaturization because the size factor  $L$  is in the denominator of eqs. (2) and (3). However, when miniaturizing the  $L$ , the increment of sensitivity has never been demonstrated. It is necessary to investigate this.

### 3. Experiments and Discussion

#### 3.1 RLG with an SOA as the gain medium

The gain medium of the conventional RLGs is He-Ne gas. Another gain medium is preferred for the novel RLG because He-Ne lasers need a high voltage source and a special glass mold to encapsulate the He-Ne gas. It is reported that the SOA can be used as a gain medium of RLGs.<sup>(11)</sup> The SOA is made of a compound semiconductor and driven by a low supply voltage. Figure 4 shows a top view of an RLG using a commercial SOA as the gain medium. The optical loop is made of invar, which is an alloy with a very small thermal expansion coefficient ( $0.1 \times 10^{-6}$  1/K). The RLG consists of an SOA (BOA 1004, Thorlabs, USA), two dielectric total reflection mirrors (BB05-E04, Thorlabs, USA), and a beam splitter (PSM95-10C05-20-1550-30 deg, SIGMA KOKI, Japan). The SOA is a module composed of an SOA chip, collimation lenses, and a Peltier device in one package. The SOA facets are coated with anti-reflection layers whose reflectance is less than 0.5%. The SOA emits light with a wavelength near 1,550 nm, and amplifies the light simultaneously. The mirrors are coated with multilayer dielectric films, and the diameter is  $\phi 12.7$  mm with  $\lambda/10$  surface flatness. The total reflection mirrors have 99.5% reflectance for a 1,550 nm laser beam. The beam splitter that also acts as the mirror for the optical circulating path is coated with multilayer dielectric films and the diameter is  $\phi 10$  mm with  $\lambda/10$  surface flatness. The beam splitter has 95% reflectance and 5% transmittance. The total floor size is  $200 \times 160$  mm<sup>2</sup> and the optical path length is 330 mm. The enclosed area,  $S$ , is 5,239 mm<sup>2</sup>. Two cubic half mirrors to divide the lights from the optical loop are assembled to measure the intensities and the wavelength spectra of the CW and CCW lasers. The reflectance and transmittance of the cubic half mirrors are both 50%. Two detectors (FDG05, Thorlabs, USA) are connected to current-to-voltage (I/V) converting circuits. The I/V circuit consists of several operational amplifiers and filters. Fiber couplers are also connected to an optical spectrum analyzer.

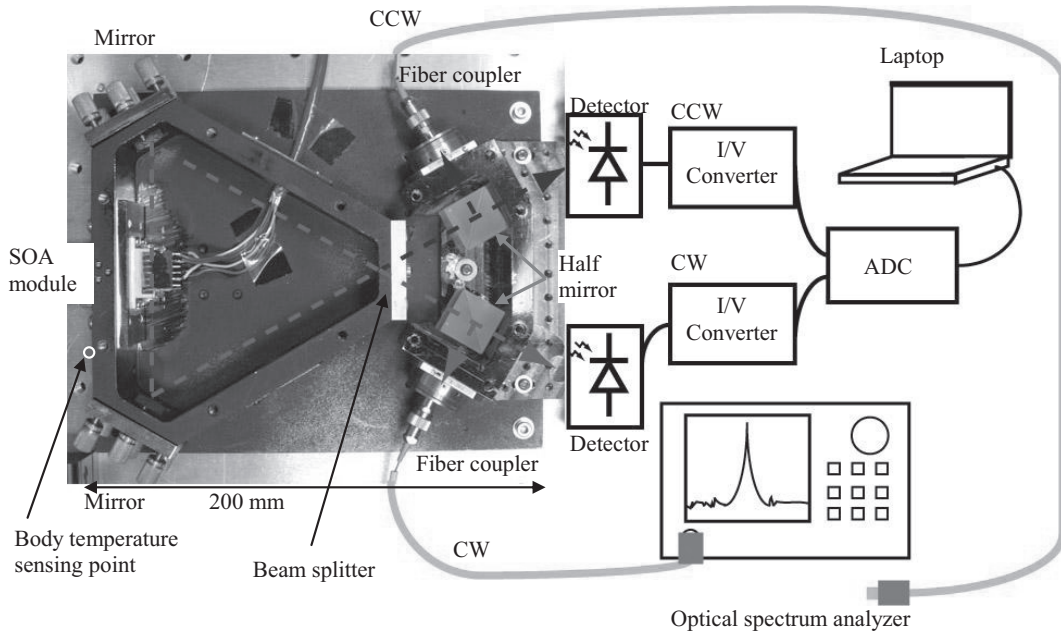


Fig. 4. RLG installed with an SOA, mirrors, and a beam splitter.

### 3.2 Basic characteristic of laser oscillation

Before observation of the winking phenomenon, the relationship between the light intensity and the injection current was measured (Fig. 5). The SOA temperature was controlled by the Peltier device under the SOA chip to  $20 \pm 0.1^\circ\text{C}$ . A well-aligned optical system with mirrors generated an oscillation in the triangular optical path. The threshold current was 48 mA. The detectors sensed almost the same intensities of the CW and CCW laser beams, simultaneously. This means that the SOA emits two counter propagating lasers. Figure 6 shows wavelength spectra for the injection current at 60 mA. The resolution of the wavelength is 20 pm. The CW and CCW lasers oscillate at the same wavelength of 1,558.10 nm. At the range of the injection current over 65 mA, the oscillation spectrum becomes unstable and multimode with mode hopping. However, the total intensities of the CW and CCW lasers are stable.

### 3.3 Observation of the winking phenomenon

The injection current of the SOA was regulated to 60 mA. The CW and CCW laser beams were oscillated at wavelengths of 1,581.10 nm at static state, and the intensities were 20.0 and 20.2  $\mu\text{W}$ , respectively. The angular velocity was applied to the RLG in a

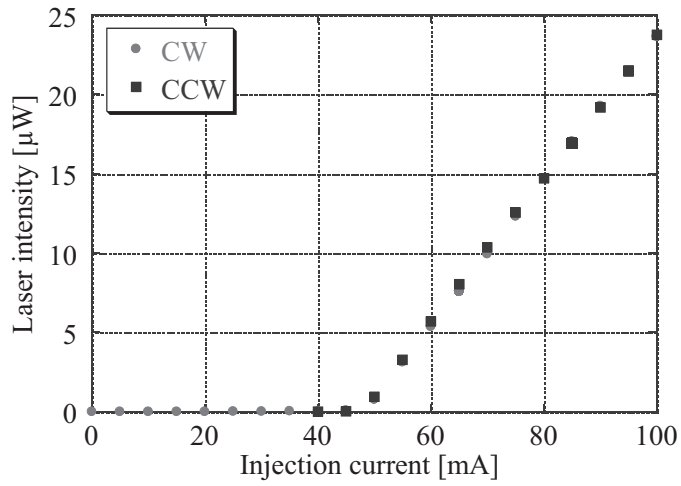


Fig. 5. Light intensity – injection current characteristics.

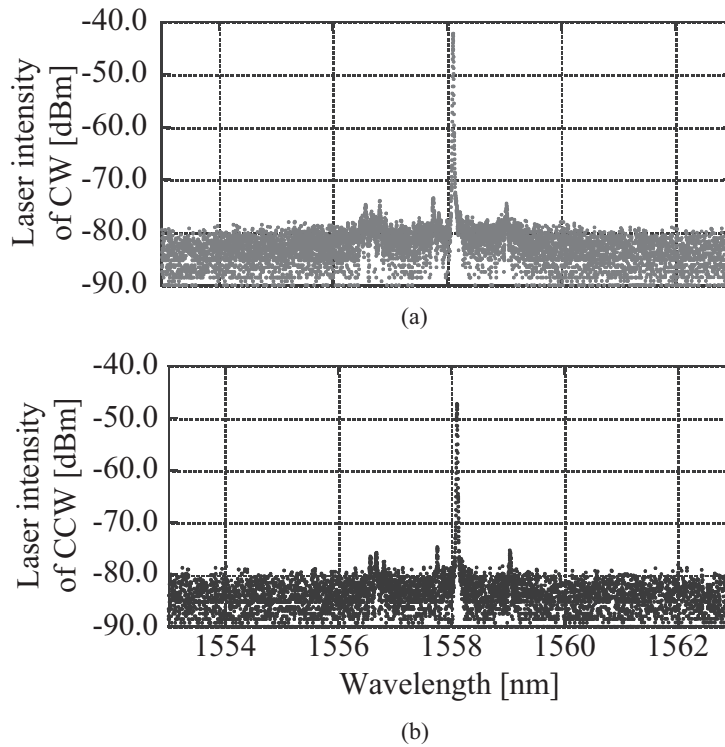


Fig. 6. External oscillating wavelength with injection current of 60 mA. (a) CW beam intensity. (b) CCW beam intensity.

range of  $\pm 120$  deg/s, and the experimental results are shown in Fig. 7. The vertical axis named “Normalized output” in Fig. 7 is the difference in intensity between the CW and CCW laser beams normalized with the intensities of the static state. The normalized output is defined by

$$\frac{I_{CCW} - I_{CW}}{I_{CCW} + I_{CW}} + \frac{I_{CCW0} - I_{CW0}}{I_{CCW0} + I_{CW0}},$$

where  $I_{CW0}$  and  $I_{CCW0}$  are the laser intensities at the static state and  $I_{CW}$  and  $I_{CCW}$  are the intensities when the angular rate is applied. The laser intensities of the CW and CCW lasers are differentially and linearly changed depending on the applied angular velocity. The intensity change of the RLG is measured to be  $1.9 \times 10^{-2} \%$ /deg/s and the nonlinearity is 0.2% in the full scale range. The change is more than 100 times larger than that of the conventional vibrating MEMS gyroscopes using Coriolis force. The current noise level was  $15.3 \text{ mV}_{p-p}$ , which corresponds to 2.6 deg/s. The improvement of the circuit to reduce the noise level is required in the future.

It was reported that the intensity change caused by the winking phenomenon depends on the injection current.<sup>(9)</sup> We attempted to increase the injection current. Figure 8 shows the influence of the injection current on the relationship between the intensity change and the applied angular velocity, for the applied angular velocity of  $\pm 600$  deg/s. At the injection current of 85 mA, the intensity change is  $6 \times 10^{-2} \%$ /deg/s. An excellent linearity in the intensity change ( $< 0.001\%$ ) is observed. The intensity change by the winking phenomenon should be nonlinear because there is a term of cosine in eqs. (2) and (3). However, the intensity change seems to be linear. The reason for this is that

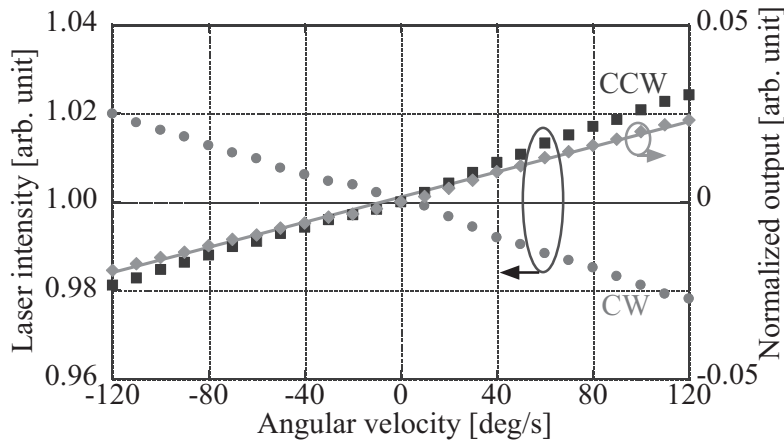


Fig. 7. Observed winking phenomenon as the detection signal for the applied angular velocity.

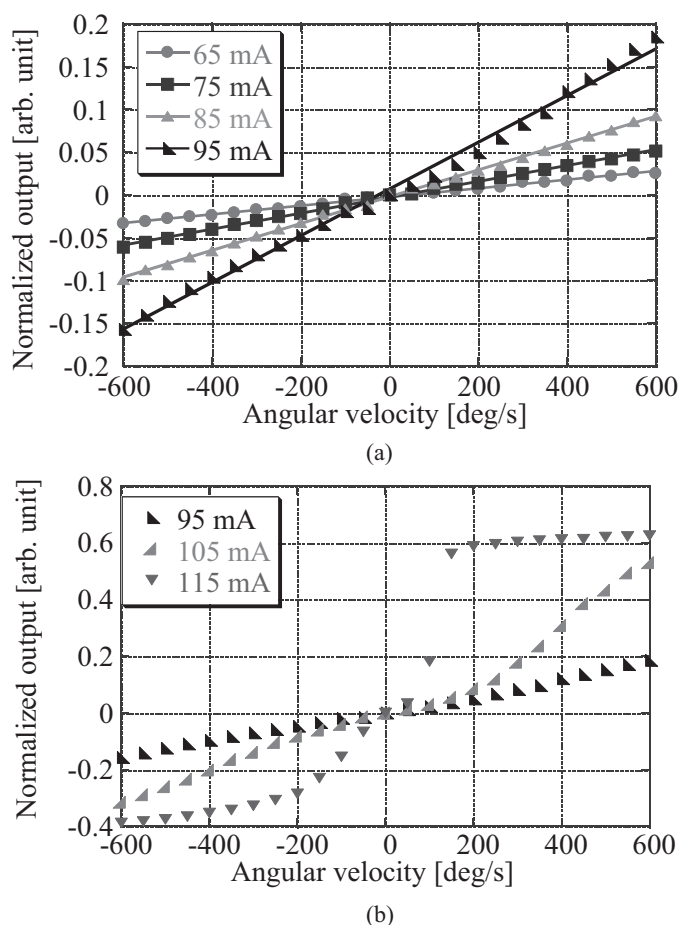


Fig. 8. Influence of the injection current on the winking phenomenon. (a) Difference in CW and CCW laser intensities normalized with the intensities of static state. The injection current of the SOA is less than 95 mA. (b) Normalized intensity change and the linearity. The injection current of the SOA is more than 95 mA.

the lock-in threshold is a higher rate than  $\pm 600$  deg/s because optical components of the RLG are optimized to miniaturize the backscattering and phase of mirrors. If applying a higher angular velocity of more than  $\pm 600$  deg/s to the RLG, nonlinear intensity change may be observed. In addition, it is confirmed that the conventional mechanical dither is not needed because the winking phenomenon is generated from 0 deg/s. From Fig. 8(a), the winking phenomenon can be applicable to gyroscopes for an injection current less than 95 mA. In Fig. 8(b), a higher injection current is applied to the SOA. Although the

characteristic is nonlinear at the range of the current over 95 mA, the intensity change becomes huge.

### 3.4 Stability

Evaluation of the stability for the RLG using the winking phenomenon is important. The stability in the time domain was measured. The measurement time was 20 min for the stability evaluation, and the injection current was regulated to 60 mA. Figure 9(a)

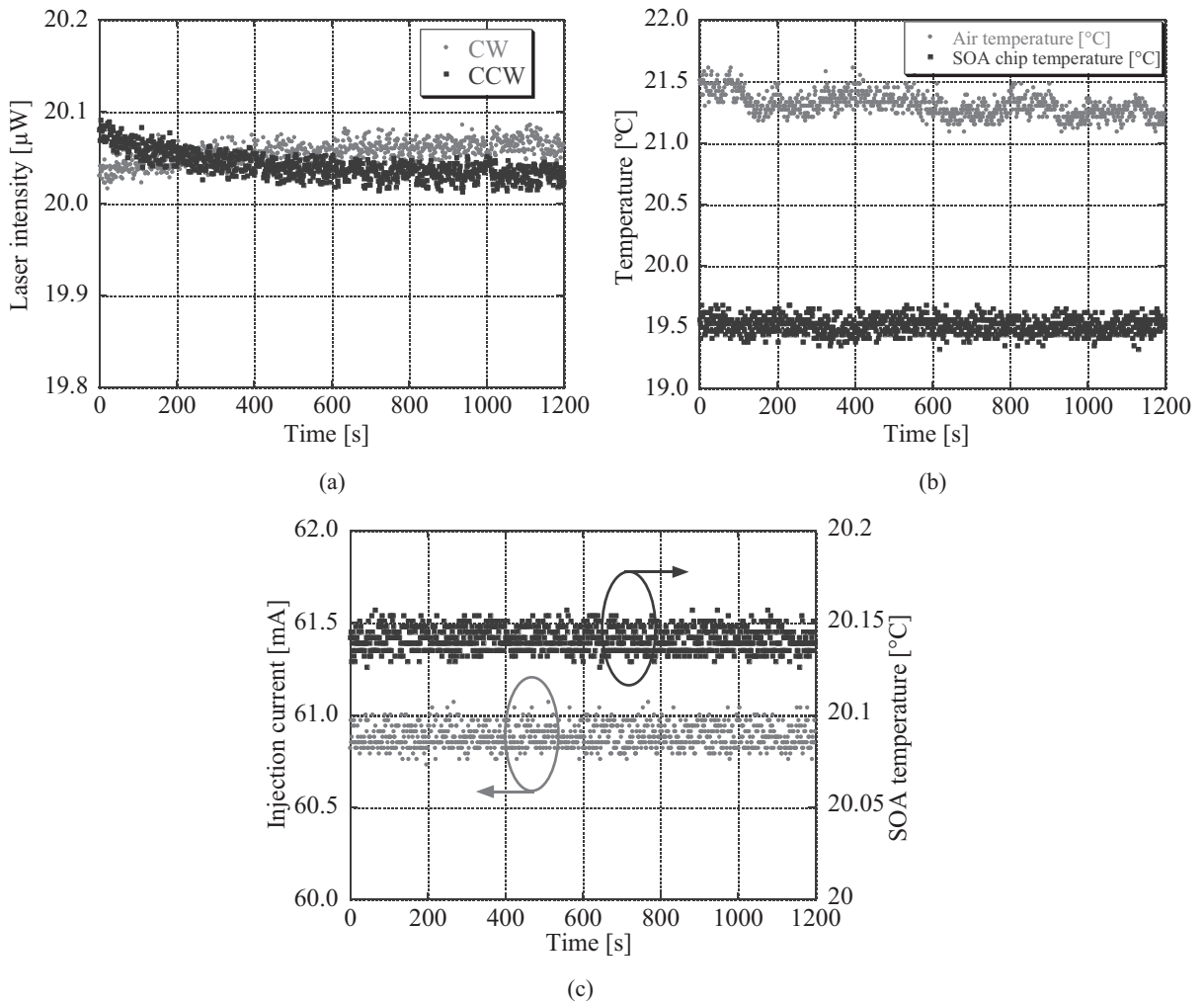


Fig. 9. Stability for 1,200 s (20 min). (a) Stability of CW and CCW intensities. (b) Temperatures of the room air and RLG (near the SOA). (c) Injection current and SOA chip temperature.

shows the intensities of the CW and CCW lasers. The intensity drift was 29.4 nW, which corresponds to the bias stability of 8.2 deg/s. Figure 9(b) shows the relationship between the air temperature and the RLG body temperature near the SOA package (shown in Fig. 3). There is a small difference between the air temperature and the body temperature because of insufficient calibration. Figure 9(c) shows the injection current, and the temperature of the SOA chip. The body and SOA chip temperatures and injection current are perfectly controlled. Figure 10 shows the influence of the body temperature of the RLG on the laser intensities. The intensity change of 0.63  $\mu\text{W}$  is observed in the 20.7 to 30.5°C range. The intensity change corresponds to a bias drift of 18.3 deg/s·°C. This bias drift may come from thermal expansion of the RLG body, mirrors, and thermal drift of the detecting circuit.

### 3.5 Future work

The absolute amplitudes of backscattering at the mirror surfaces and the phase when the laser beams backscattered are important to theoretically estimate the intensity change caused by the winking phenomenon. However, the measurement of those characteristics is rather difficult and the theoretical analysis of the winking phenomenon is still being performed. Explained in § 2.3, the dependence of  $L$  on the intensity change of the winking phenomenon has yet to be demonstrated. In addition, the stability of the RLG should be improved by controlling the temperature and miniaturizing the RLG because the current RLG is influenced by temperature conditions.

## 4. Conclusions

In this paper, we proposed a novel sensing method of angular velocity using the winking phenomenon originated from the Sagnac effect, which is the intensity change

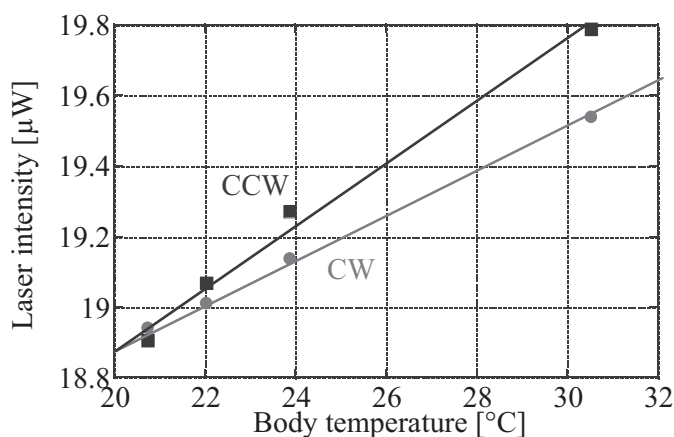


Fig. 10. Influence of the body temperature on the output.

of laser beams depending on the applied angular velocity. An RLG was assembled using an SOA as the gain medium, mirrors, and a beam splitter to observe the winking phenomenon. By suitable alignment of the mirrors, the CW and CCW lasers were simultaneously generated. The intensities and wavelengths were the same between the CW and CCW lasers at the static state. The intensity change is  $4 \times 10^{-2} \%$ /deg/s at the injection current of 60 mA when an angular velocity is applied in the range of  $\pm 120$  deg/s. The intensity change is more than 100 times larger than that of the conventional vibrating MEMS gyroscopes. The injection current should be chosen to be less than 95 mA for the sufficient linearity of 0.2%. An advantage compared with conventional RLGs is confirmed in that the mechanical dither is not required for the RLG sensing the winking phenomenon because the winking phenomenon is observed from the static state. The stability was measured in 20 min. A bias drift of 8.2 deg/s is observed. The influence of temperature is 18.3 deg/s/°C. Miniaturization and control of the temperature of the RLG will improve the stability of the RLG. In conclusion, the RLG using the winking phenomenon is available.

### Acknowledgment

We gratefully acknowledge members of the ERATO Maenaka Human-Sensing Fusion Project sponsored by Japan Science and Technology Agency for their valuable comments and stimulating discussions.

### References

- 1 K. Liu, W. Zhang, W. Chen, K. Li, F. Dai, F. Cui, X. Wu, G. Ma and Q. Xiao: *J. Micromech. Microeng.* **19** (2009) 113001.
- 2 Analog Devices Inc. ADRXS300 datasheet.
- 3 S. E. Alper and T. Akin: *Sens. Actuators, A* **115** (2004) 336.
- 4 S. Ioku, H. Araki, H. Kohara, T. Fujita, K. Maenaka and Y. Takayama: *IEEJ Trans. SM.* **125** (2005) 337.
- 5 D. Tsai and W. Fang: *Sens. Actuators, A* **126** (2006) 33.
- 6 M. Saukoski, L. Aaktonen, T. Salo and K. Halonen: *Sens. Actuators, A* **147** (2008) 183.
- 7 A. Lawrence: *Modern Inertial Technology*, 2nd ed. (Springer-Verlag, New York, 1998) p. 72.
- 8 Haneywell International Inc. GG1320AN01 datasheet.
- 9 F. Aronowitz and R. J. Collins: *J. Appl. Phys.* **41** (1970) 130.
- 10 I. Kataoka and Y. Kawahara: *Jpn. J. Appl. Phys.* **25** (1986) 1365.
- 11 T. Hashimoto, K. Makimura, K. Kanda, T. Fujita and K. Maenaka: *IEEJ Sec. E* **131** (2011) 154.

**About the Authors**

**Taichi Hashimoto** received his B. E. and M. E. degrees from the Himeji Institute of Technology in 2006 and the University of Hyogo in 2009, respectively. Currently, he is a Ph. D. candidate researching MEMS-RLG.



**Kenichi Makimura** received his B. E. in electrical engineering from the University of Hyogo, Japan, in 2011. Since 2011, he has been a Master's student at the University of Hyogo. Currently, he is researching MEMS-RLG.



**Kensuke Kanda** received his B. E., M. E., and Dr. degrees in mechanical engineering from Tokyo Metropolitan University, Japan, in 2000, 2003, and 2006, respectively. From 2006 to 2008, he worked as a postdoctoral researcher in the Advanced Software Technology and Mechatronics Research Institute of Kyoto, Japan. From 2008 to 2010, he worked for the Maenaka Human-Sensing Fusion Project at Japan Science and Technology Agency, Japan. Since 2010, he has been an Assistant professor in the Department of Electrical Engineering and Computer Sciences, the University of Hyogo. His research interests include microfluidic devices, piezoelectric microdevices, accelerometers, force sensors, power harvesters, and their integration.



**Takayuki Fujita** received his B. E., M. E., and Ph. D. degrees from the Himeji Institute of Technology, Japan, in 1995, 1997, and 2000, respectively. Since 2001, he has been a Research Associate at the Himeji Institute of Technology. He is currently an associate professor in the Department of Electrical Engineering and Computer Sciences, the University of Hyogo. His research topics are MEMS and integrated circuit devices.



**Kazusuke Maenaka** received his B. E., M. E., and Ph. D. degrees from Toyohashi University of Technology, Japan, in 1982, 1984, and 1990, respectively. Since 1993, he has been with the Department of Electronics at the Himeji Institute of Technology. With the unification of universities in the Hyogo prefecture in April 2004, he joined the University of Hyogo, where he is presently a professor. Since 2008, he has been the project leader of the Maenaka Human-Sensing Fusion Project supported by the Japan Science and Technology Agency. His research interests include MEMS devices and technology, especially silicon mechanical sensors and their integration.